Physical Model and Dynamic Equations

MEMS Piezoelectric Vibrational Energy Harvesting Lab

Jorge Mario Monsalve Guaracao[1]

Contents

[1]BS Mechanical & Electronics Engineering. Universidad de los Andes. jm.monsalve886@uniandes.edu.co. Undergraduate researcher at the nanoHUB SURF program, Purdue University.

Introduction

This *nanoHUB.org* tool is intended to simulate the dynamical behavior of a MEMS piezoelectric energy harvesting device. These devices use the principle of the direct piezoelectric effect to convert the energy of a vibrating surface into an electrical current. This is done by shaking a cantilevered beam which is coupled to a piezoelectric film. As the vibration bends the beam, the piezoelectric material accumulates electrical charge and delivers it to a circuit. The equations that are used to model this system are the mechanical force balance, along with Kirchhoff's laws for the harvesting circuit; which interact with each other thanks to the piezoelectric coefficients.

Description of the Device

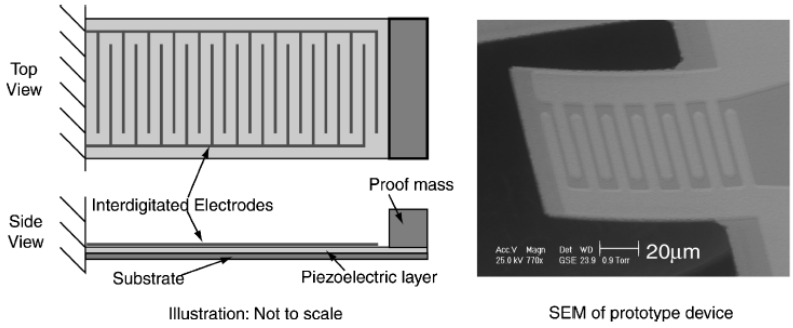

Figure 1 Picture of a MEMS piezoelectric bimorph. ***Source: duToit et al (2005)***

Figure 1 shows a picture of a typical MEMS piezoelectric *unimorph* beam. This device consists of a piezoelectric film with its corresponding electrodes, a substrate and a proof mass. Each of them accomplishes a specific function. The piezoelectric film (usually made from PZT or AlN) creates electrical charge as it bends and delivers it to the interdigitated electrodes. The substrate (usually metallic) provides stiffness to the beam; and the proof mass helps to increase the inertial forces and lower the resonance frequency of the device. It is interesting that all these features are constructed in the scale of millimeters or even tens of micrometers.

General Physical Model

The dynamics of this device can be derived by understanding it from two different perspectives: mechanical and electrical. From the mechanical perspective it can be considered as a classical mass-spring-damper system with an additional term concerning the electrical force induced by the piezoelectric. From the electrical point of view, the device is considered a linear circuit with a parallel-plate capacitor that models the piezoelectric, a current source regarding the injected charge and a resistive load for dissipating the electrical power. Under these assumptions the dynamics of the cantilever can be modeled with the system of ordinary differential equations shown below.

$$m_{eq}\ddot{z} + c_{eq}\dot{z} + k_{eq}z + \theta_1 V = -m_{eq}(K\ddot{y}) + c_{air}(K\dot{y})$$

$$\theta_2 \dot{z} = \dot{V} + \frac{V}{R_L C_p}$$

Where

- m_{eq}: Equivalent inertia of the beam and proof mass.
- c_{eq}: Equivalent mechanical damping
- c_{air}: Equivalent mechanical damping (only concerning air resistance)
- k_{eq}: Equivalent stiffness of the beam
- θ_1: Force induced by the piezoelectric (backward electromechanical coupling)
- θ_2: Charge induced by the piezoelectric (forward electromechanical coupling)
- V: Voltage between the electrodes
- R: Total resistive load
- z: Displacement of the beam's tip relative to the frame
- y: Displacement of the frame (vibrations source)
- K: Lumped-parameter correction factor.

Dynamic Force Balance

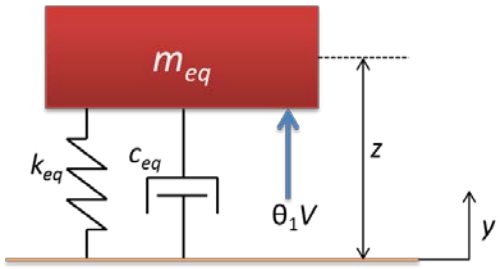

Figure 2 Equivalent mass-spring-damper mechanical model

In this simulation program an approximation is used to predict the displacement of the tip of the cantilever. Formally speaking, an elastic beam can be precisely modeled with a partial differential equation that allows calculating its shape at any instant of time. However, in this simulation program an ordinary differential equation is used to compute just the displacement of the tip of the beam. This is called the lumped-parameter modeling on which the interaction of the tip with the rest of the structure is replaced by a set of equivalent parameters. As a result, only the first oscillation mode of the cantilever is predicted in this mode; therefore, the simulations of this tool will be valid only for frequencies below or close to the first resonance of the structure. Nonetheless, these are the kind of oscillations from which more energy can be harvested. For this model to hold, it is important for the proof mass to be greater than the mass of the beam itself. If the ratio of the end-mass to the mass of the layers is low a correction factor must be used, as stated by (Erktug, 2009), which is considered in the program. Even with this approximation, the latter assumptions are valid for most harvesting applications, and by using this model the simulation will be considerably faster.

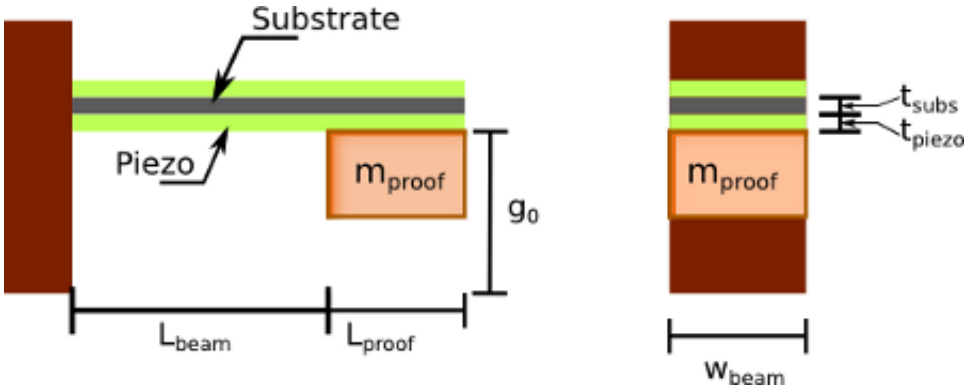

Figure 3 Schematic of the geometry of the cantilevered beam

Equivalent mass

The total inertia of the system is given by the Lord Rayleigh approximation, which states

$$m_{eq} = \frac{33}{140} m_{beam} + m_{proof}$$

This accounts the effect of the mass of the beam, which is much less compared to the contribution of the proof mass.

Equivalent Stiffness

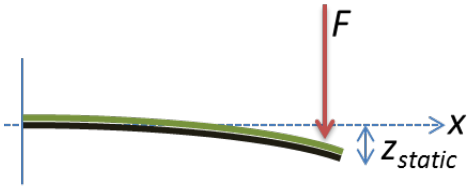

Figure 4 Schematic of the deflection of the beam

According to the Euler-Bernoulli beam theory, the static displacement of the tip for a concentrated force at that point in a cantilever is given by

$$z_{static} = \frac{{L_{eff}}^3}{3c_{11}\, I_{eff}} F = \frac{F}{k_{eq}}$$

The stiffness of the beam is given both by the geometry and the material's properties. Here the effective length is considered to be $L_{eff} = L_{beam} + 0.4L_{proof}$ taking into account that the seismic mass would occupy some space. The latter expression was found empirically by (Andosca, McDonald, Genova, Rosenberg, & Keating, 2012) as a correction to the traditional approach of $L_{eff} = L_{beam} + 0.5L_{proof}$.

Since the device consists of two materials, the moment of inertia of the cross-section will be found with the transformed section method

$$I_{eff} = I_p + \left(\frac{Y_s}{c_{11}}\right) I_s = I_p + nI_s$$

Where

- I_{eff}: Effective area moment of inertia
- I_s: Moment of inertia of the substrate's cross section
- I_p: Moment of inertia of the piezoelectric's cross section
- Y_s: Young's modulus for the substrate
- c_{11}: Young's modulus for the piezoelectric (1- direction)
- n: Elastic modulus ratio

Solution for a Unimorph device

If the beam is built from only one piezoelectric layer and one metallic layer the device is called a *Unimorph*. When calculating the moment of inertia it is important to take into account that the neutral axis does not necessarily rely in the center of the beam. It is found by the relationship

$$Y_s \int_s ydA_s + c_{11} \int_p ydA_p = 0$$

Solving for the y-coordinate which allows the integrals to cancel each other gives the position of the neutral axis with respect to the border of the substrate layer as[2]

$$y_{neut} = \frac{\frac{1}{2}nt_s^2 + \left(t_s + \frac{1}{2}t_p\right)t_p}{nt_s + t_p}$$

Once the position of the neutral axis is known the moments of inertia can be calculated through the parallel-axis theorem

$$I_p = \frac{wt_p^3}{12} + wt_p\left(t_s + \frac{1}{2}t_p - y_{neut}\right)^2$$

$$I_s = \frac{wt_s^3}{12} + wt_s\left(y_{neut} - \frac{1}{2}t_s\right)^2$$

Solution for a Bimorph device

In the case that two piezoelectric layers are used in a sandwich-like arrangement the device is called a *Bimorph*. In this setup the symmetry simplifies some calculations as the neutral axis would rely approximately at the center of the beam (it will be assumed that the piezoelectric layers have exactly the same thickness). Applying the same parallel-axis theorem in this case yields

$$I_p = 2\left(\frac{wt_p^3}{12} + wt_p\left(\frac{1}{2}t_p + \frac{1}{2}t_s\right)^2\right)$$

[2] Another (more intuitive) way to calculate this coordinate is to find the centroid of the cross-section, taking into account that the width of the substrate layer has to be multiplied by the factor *n*.

$$I_s = \frac{wt_s^3}{12}$$

Equivalent Damping

The damping term "c_{eq}" accounts all energy losses due to friction in the system. In this case, it is more convenient to express the mechanical damping in terms of the dimensionless damping ratio as follows

$$\frac{c_{eq}}{m_{eq}} = 2\zeta\omega_n$$

Where ζ is the damping ratio; and $\omega_n = \sqrt{k_{eq}/m_{eq}}$ is the natural frequency. duToit *et al* (2005) provide expressions to calculate the ζ factor, superposing different means of mechanical energy dissipation as follows

$$\zeta = \zeta_{drag} + \zeta_{squeeze} + \zeta_{struct} + \zeta_{support}$$

- $\zeta_{drag} = \frac{3\pi\mu w + \frac{3}{4}\pi w^2\sqrt{2\rho_{air}\mu\omega}}{2\rho_{beam}wlh\omega}$
- $\zeta_{squeeze} = \frac{\mu w^2}{2\rho_{beam}g_0^3 h\omega}$
- $\zeta_{struct} = \eta/2$
- $\zeta_{support} = 0.23h^3/l^3$

These expressions are derived in the work of (Hiroshi, Kiyoshi, & Susumo, 1994) on which the device is modeled as a rectangular prismatic beam of length l, width w and thickness h. The other several variables to calculate the damping include the density and viscosity of air (ρ_{air}, μ), the structural damping (η), the gap between the beam and the support (g_0) and the operating frequency (ω). Although the calculation of damping includes many terms, all of them affect the performance. From these expressions, the most predominant is usually the structural damping; however, at small scales the other terms become important.

Now, for the user it wouldn't be comfortable to figure out the current air density and viscosity. These variables depend on the local atmospheric pressure and ambient temperature, which are more likely to be known. Therefore, the tool uses an empirical model (Power-Law Viscosity law) and the ideal gas model to calculate these variables as follows

$$\mu = 1.716 \times 10^{-5}\left(\frac{T}{273K}\right)^{\frac{2}{3}} kg/(m-s)$$

$$\rho_{air} = \frac{P}{RT}$$

Lumped-Parameter Correction Factor

As Erktug (2009) explains, a more formal modeling of the dynamics of the beam would be to consider it a continuous 1-D system. Nonetheless, the simplified lumped parameter model can be corrected by multiplying the output by a correction factor that depends on the relationship between the proof mass

and the beam's mass. If the m_{proof}/m_{beam} ratio is very large, this correction factor will tend to 1 since all the inertia would be actually concentrated in the tip of the beam. His correction formula is given by the expression

$$\frac{z_{actual}}{z_{lumped}} = K = \frac{\left(\frac{m_p}{m_b}\right)^2 + 0.603\left(\frac{m_p}{m_b}\right) + 0.08955}{\left(\frac{m_p}{m_b}\right)^2 + 0.4637\left(\frac{m_p}{m_b}\right) + 0.05718}$$

Piezoelectric Electromechanical Coupling

The piezoelectric film is the responsible element for the electromechanical interaction. From the electrical point of view, the piezoelectric is storing charge as it is being deformed; therefore it can be modeled as a capacitor with a current source that imbues some charge to it because of the mechanical strain. This is called the *direct* piezoelectric effect and it is accounted in the electrical circuit equation. On the other hand, the fact that an electric field emerges in the electrodes means that a force is also being exerted on the mechanical structure because of the *converse* piezoelectric effect. This force happens to be proportional to the output voltage and affects the dynamic force balance with the backward coupling term. The derivation of these terms is based on the work of (Erktug, 2009) but adapted to the lumped parameter model presented here.

Backward Electromechanical Coupling

The piezoelectric film itself doesn't exert a punctual force on the tip of the beam. Rather, an internal strain is developed because of the electric field that is present within the material. Nevertheless, it is possible to find an equivalent force located at the tip of the beam (as in figure 4) that could compensate the stress provoked by the converse piezoelectric effect. In order to do this, it is necessary to apply the superposition principle. Let δ be the total displacement at the tip caused both by the applied force and voltage, which can be added linearly. The equivalent blocking force would set the total displacement to zero, that is

$$\delta = \delta(V) + \delta(F) = 0 \rightarrow \delta_V = -\frac{F_{block}}{k_{eq}}$$

Now, the voltage-to-displacement relationship is not straightforward. First it is necessary to consider how the voltage in the material causes a stress, which itself exerts a bending moment on the beam. Once the bending moment is found, the Euler-Bernoulli law can be used to find the deflection in terms of the voltage. It will be shown that the piezoelectric films apply a constant moment along the beam (Erktug, 2009) (Townley), therefore the deflection will be given by[3]

$$\delta(V) = \frac{M(V)}{c_{11}I_{eff}}\frac{L^2}{2}$$

[3] For more reference on elastic beam deflection see
http://ruina.tam.cornell.edu/Courses/ME4730/Rand4770Vibrations/BeamFormulas.pdf

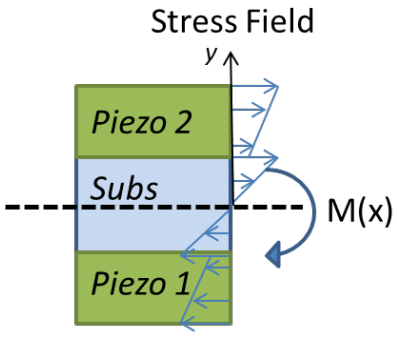

Figure 5 Stress field in a cross section of the beam

As illustrated in Figure 5, a bending moment will result according to the stress field across the beam in the following way

$$M(x) = w\int_{piezo1}\sigma_p y dy + w\int_{subs}\sigma_s y dy + w\int_{piezo2}\sigma_p y dy$$

In this case, only the external stress caused by the piezoelectric is being considered hence the term regarding the stress in the substrate is zero. In the piezoelectric films, though, it varies linearly with the electric field in the following way[4]

$$\sigma_p = c_{11}d_{31}E_3$$

As it can be seen, the bending moment depends on the geometry and number of piezoelectric layers (unimorph/bimorph). Also, as stated by (Erktug, 2009) (Roundy, 2003) it happens to be affected by the type of connection of the layers (series/parallel) since the electric field (E_3) would be different. Calculating the integral yields the following results for each different case (explained in more detail by (Erktug, 2009) for the bimorph case).

Unimorph device

$$M(V) = c_{11}d_{31}\frac{w}{2t_p}\left[\left(t_p + t_s - y_{neut}\right)^2 - \left(t_s - y_{neut}\right)^2\right]V$$

Bimorph – Parallel connection:

$$M(V) = c_{11}d_{31}\frac{w}{t_p}\left[\left(t_p + \frac{t_s}{2}\right)^2 - \left(\frac{t_s}{2}\right)^2\right]V$$

Bimorph – Series connection *(Vs = Vp/2)*:

$$M(V) = c_{11}d_{31}\frac{w}{2t_p}\left[\left(t_p + \frac{t_s}{2}\right)^2 - \left(\frac{t_s}{2}\right)^2\right]V$$

[4] In this tool the signs are adjusted in the coefficients of the differential equation to avoid confusions to the user. Here the **absolute value** of the d31 coefficient is used. The tool will ask the user to insert a positive value for d31.

After finding the bending moment, finally a relationship between the voltage and the deflection can be found. After arranging the equations, the equivalent force per unit voltage that the piezoelectric would apply for each of the cases is found as

$$\theta_1^{unimorph} = k_{eq} d_{31} \left\{ \frac{w L_{eff}^2}{4 t_p I_{eff}} \left[\left(t_p + t_s - y_{neut} \right)^2 - \left(t_s - y_{neut} \right)^2 \right] \right\}$$

$$\theta_1^{parall} = k_{eq} d_{31} \left\{ \frac{w L_{eff}^2}{2 t_p I_{eff}} \left[\left(t_p + \frac{t_s}{2} \right)^2 - \left(\frac{t_s}{2} \right)^2 \right] \right\} = 2\theta_1^{series}$$

Forward Electromechanical Coupling

The most important aspect of the MEMS piezoelectric generator is its capability to deliver an electric current because of the stress it is subject to. Because of the direct piezoelectric effect, the electric displacement inside the material caused only by the mechanical stress is given by

$$D_3 = d_{31} \sigma_1$$

This relationship holds for an infinitesimal element of the film. To find the total electric charge generated because of the strain, it is necessary to integrate over all the film along the 3-direction and use Hooke's law as follows

$$Q = (N_{layers}) \int D_3 dA_3 = (N_{layers}) w L_b d_{31} c_{11} \varepsilon_{avg}$$

Now, it is necessary to find the average strain along the whole beam. Again, it is necessary to consider here that a punctual load is being applied at the tip of the cantilever to find the stress distribution. With this assumption, the average stress can be found by applying the flexure-formula in this way

$$\varepsilon_{avg} = \frac{1}{L_{eff}} \int_0^{L_{eff}} \frac{M(x) c_{neut}}{c_{11} I_{eff}} dx = \frac{1}{L_{eff}} \int_0^{L_{eff}} \frac{F(L_{eff} - x) c_{neut}}{c_{11} I_{eff}} dx = \frac{F L_{eff} c_{neut}}{2 c_{11} I_{eff}} = \left(\frac{3 c_{neut}}{2 L_{eff}^2} \right) \underbrace{\frac{F}{k_{eq}}}_{z_{static}}$$

Here c_{neut} corresponds to the distance from the center of the piezoelectric film to the neutral axis. Merging the last equations it is possible to find the electric charge that results from deflecting the beam with a punctual load. Notice that the average strain was found as an approximation of the case when a static load is applied at the tip, as suggested in (Roundy, 2003).

$$Q(t) = \left(N_{layers} \right) w L_b c_{11} d_{31} \left(\frac{3 c_{neut}}{2 L_{eff}^2} \right) z(t)$$

As a final step, the electric current can be found by differentiating the last expression

$$i(t) = (N_{layers})c_{11}d_{31}wL_b\left(\frac{3c_{neut}}{2L_{eff}^2}\right)z'(t) = qz'(t)$$

The term N_{layers} has to be applied with care. It will be two in the parallel case only, for in this connection both capacitors store charge independently. In the series case; however, the injected current is the same for both layers according to Kirchhoff's current law hence electrically speaking it counts as just one layer (Roundy, 2003).

Electrical Circuit Model

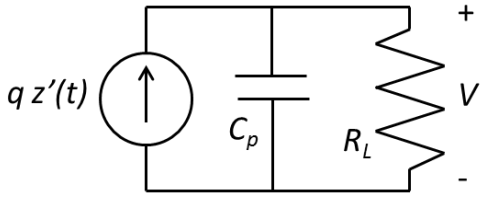

Figure 6 Circuital models for the linear case

In the previous sections, the mechanical balance of the device was studied, as well as the electromechanical coupling that arises because of the piezoelectric effect. Now, the circuital equations will be derived to calculate the useful electrical power that is generated.

From the electrical point of view, the MEMS harvesting system can be understood as linear RC circuit. In this case, the piezoelectric will be replaced by a parallel-plate capacitor since it is an element that stores charge. The forward electromechanical coupling will be represented as a current source, which would be the powering element for the electrical circuit. This power can be delivered to a resistor, or a full-wave rectifier circuit, which will be analyzed later. For the resistive load, applying KCL gives

$$\frac{dV_{out}}{dt} = \frac{q}{C_p}\dot{z} - \frac{V_{out}}{R_L C_p} = \theta_2\dot{z} - \frac{V_{out}}{R_L C_p}$$

Piezoelectric Capacitance

Because of the transverse piezoelectric coefficient (d_{31}), the strain in the longitudinal ("1") direction will cause an electric displacement in the transverse ("3") direction. Therefore, the piezoelectric film can be viewed as a parallel-plate capacitor with an active area of $w \times L_{eff}$. This approach is valid in the low-frequency region (far below the GHz band). The capacitance of a single piezoelectric layer will thus be

$$C_p^{unimorph} = e_{33}^S\frac{wL_{eff}}{t_p}$$

Where e_{33} is the electrical permittivity of the material at constant strain, that is: $e_{33}^S = e_r^T\varepsilon_0 - d_{31}^2c_{11}$ in the plain-stress approximation (Erktug, 2009). It is important to note that the program simply receives an input for the *relative permittivity*: it will be assumed that the user will specify the correct permittivity and internally it is multiplied by ε_0.

For the bimorph case, the capacitance also changes according to the connection in the following way

$$C_p^{parallel} = 2e_{33}^S \frac{wL_{eff}}{t_p}$$

$$C_p^{series} = e_{33}^S \frac{wL_{eff}}{2t_p}$$

Full-Wave Rectifier Circuit

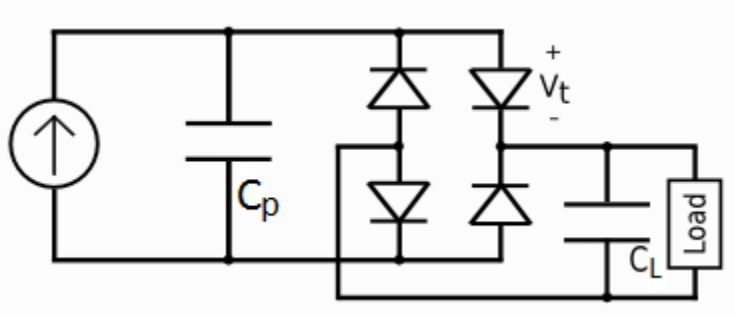

Figure 7 Schematic of the full-wave rectifier circuit

The simple case of dissipating the scavenged energy into a resistor is of no practical use, although it is very useful for characterization purposes. One of the circuit topologies used in these cases consists of a full wave rectifier connected to an output capacitor and a dissipating element (electrical load). The diode bridge allows converting the input AC voltage into a DC voltage with a small ripple. This is a nonlinear circuit and for the solution method of this tool it will be assumed that the diodes perform as ideal switches, with some small threshold voltage (which could be in the order of 0.3 to 0.7 V). Of course, again there has to be some passive element to deliver the energy to, and a resistor is used as load in the equations (otherwise, the capacitor would keep charging indefinitely).

In order to solve this circuit, three cases must be considered according to the state of the diodes. The first case would be when the input voltage is not enough to activate none of the diodes thus the load would be disconnected from the source. The second case would be when the input voltage is positive enough to allow current to pass to the load through two of the diodes. The other case would be when the input voltage is negative enough to allow current to pass to the load through the two remaining diodes. The latter cases ensure that the output voltage is always positive, and each one represents a different dynamic equation. As there are two energy storage elements (namely C_p and C_L) there will be two state variables regarding the electrical circuit, instead of one as in the case of the simple resistive load.

Case 1: Diodes OFF

Since the output is uncoupled, there are only two equations for the RC output circuit and the input capacitor being charged by the current source

$$\frac{dV_p}{dt} = \frac{1}{C_p} i(t) = \theta_2 z'(t)$$

$$\frac{dV_{out}}{dt} = -\frac{V_{out}}{R_L C_L}$$

In order for the system to remain in this case, it must be checked that

$$|V_p| < 2V_t + V_{out}$$

Case 2: Positive half-cycle

In this case, two of the diodes turn ON and there is a voltage drop from the input because of the threshold voltage, that is

$$V_{out} = V_p - 2V_t$$

The input current now is delivered to two capacitors and the resistive load, hence by KCL

$$qz'(t) = C_p \frac{dV_p}{dt} + C_L \frac{dV_{out}}{dt} + \frac{V_{out}}{R_L}$$

The equations for the two state variables would be

$$\frac{dV_p}{dt} = \frac{\theta_2}{1 - C_L/C_p} z'(t) - \frac{V_{out}}{R_L(C_L + C_p)}$$

$$\frac{dV_{out}}{dt} = \frac{\theta_2}{1 - C_L/C_p} z'(t) - \frac{V_{out}}{R_L(C_L + C_p)}$$

Notice that the coefficients are exactly the same for both variables. However, it is important to distinguish them because both voltages are very likely to be different. For the system to remain in this case it must be checked that the current through the diodes is positive. However, just by verifying that both the input voltage is positive and higher than the threshold barrier of the diodes this would be accomplished.

Case 3: Negative half-cycle

The last case would be when the injected current changes its sign, charging the piezoelectric with an opposite voltage than the previous case. Here, the relationship between input and output voltages changes

$$V_{out} = -V_p - 2V_t$$

Compared to the last case, only some signs change in the differential equations, which would be

$$\frac{dV_p}{dt} = \frac{\theta_2}{1 - C_L/C_p} z'(t) + \frac{V_{out}}{R_L(C_L + C_p)}$$

$$\frac{dV_{out}}{dt} = -\frac{\theta_2}{1 - C_L/C_p} z'(t) - \frac{V_{out}}{R_L(C_L + C_p)}$$

Resonance Frequencies

In the design of a mechanical system subject to dynamic loads it is highly important to predict its resonance frequencies. Unlike most cases in structure design, here resonance is desired and it is critical for the device to operate very close to the resonance frequency in order to scavenge enough power. In continuous beams there are virtually infinite resonance frequencies according to each mode of oscillation. However, as the single-mode approximation was adopted here only one resonance frequency will be predicted by the simulation program which corresponds to the first oscillation mode. Again, this is very reasonable for most of the cases since vibrations with enough amplitude are always found in the low-frequency band.

The resonance frequency of this system depends both on the mechanical structure and the electrical load (Erktug, 2009) (duTout, Wardle, & Kim, 2005). Depending on the load resistance, the resonance frequency will shift slightly, for this reason one can speak of a "short circuit" resonance and an "open circuit" resonance. This can be derived by transforming the dynamic equations into the Laplace domain (of course, for the case with no rectifier) which, after some algebraic manipulation, yields the following voltage-to-acceleration transfer function

$$\frac{V(s)}{A(s)} = \frac{-\theta_2(c_{air}+s)/m}{s^3 + \left(2\zeta\omega_n - \frac{1}{RC}\right)s^2 + \left(\omega_n^2 + \frac{\theta_1\theta_2}{m} - \frac{2\zeta\omega_n}{RC}\right)s - \frac{\omega_n^2}{RC}}$$

Finding the exact resonance frequency for any case of load resistance yields a rather tedious expression. Moreover, the change is only significant for large resistance shifts. Instead of this, a common practice is to specify the resonance for the short circuit and open circuit cases, taking the limit when $R \to 0$ and $R \to \infty$ respectively. This gives the following cases

$$\left.\frac{V(s)}{A(s)}\right]_{sc} \approx \frac{(RC)\theta_2\,(c_{air}+s)/m}{s^2 + 2\zeta\omega_n s + \omega_n^2}$$

$$\left.\frac{V(s)}{A(s)}\right]_{oc} \approx \frac{-\theta_2\,(c_{air}+s)/m}{s\left(s^2 + 2\zeta\omega_n s + \left(\omega_n^2 + \frac{\theta_1\theta_2}{m}\right)\right)}$$

Now, since this is a mechanical system excited from its base, it is known that the frequency for peak displacement (or in this case, voltage) will be the related to the term in the second order pole without a power of *s*. That is,

$$\omega_{sc} = \omega_n$$

$$\omega_{oc} = \sqrt{\omega_n^2 + \frac{\theta_1\theta_2}{m}}$$

Numerical solution

Once the differential equations of the system are stated, a numerical method can be implemented to solve the state variables along the time-span of the simulation. This nanoHUB tool implements the 4th order *Runge-Kutta* algorithm. This method is fast and accurate, and has a constant time step, which allows to make frequency analysis with the results. For this algorithm to be implemented, the equations have to be written in matrix form. The state variables of this system would be $z, \dot{z}, V_p$ and V_{out}. Arranging all the equations yields the following[5]

$$\frac{d}{dt}\begin{bmatrix} z \\ \dot{z} \\ V_p \\ V_{out} \end{bmatrix} = \begin{bmatrix} 0 & 1 & 0 & 0 \\ -\frac{k_{eq}}{m_{eq}} & -\frac{c_{eq}}{m_{eq}} & -\frac{\theta_1}{m_{eq}} & 0 \\ 0 & \frac{\theta_2}{1+\frac{C_L}{C_p}} & 0 & -\frac{1}{R_L(C_L+C_p)} \\ 0 & \frac{\theta_2}{1+\frac{C_L}{C_p}} & 0 & -\frac{1}{R_L(C_L+C_p)} \end{bmatrix}\begin{bmatrix} z \\ \dot{z} \\ V_p \\ V_{out} \end{bmatrix} + \begin{bmatrix} 0 & 0 \\ -\frac{c_{air}}{m_{eq}} & -1 \\ 0 & 0 \end{bmatrix}\begin{bmatrix} \dot{y} \\ \ddot{y} \end{bmatrix}$$

Or, in a summarized way

$$\frac{d}{dt}\vec{x} = A\vec{x} + B\vec{y}$$

Physically speaking, this would be enough to solve the differential equations. Nonetheless, from a more computational point of view there is a high risk for this equation to become *stiff* depending on the values of the coefficients. This could happen if the time step is not small enough in comparison to the natural period of the mechanical structure or the RC time constant, among many other possible causes. If the equation becomes stiff, the derivatives are highly over-estimated and the state variables could take unreasonable values in the order of 10^{200}. To avoid this, and allow the user to design devices within a wide range of dimensions (covering the micro-scale to millimeter-scale), the equations are internally solved in a dimensionless form.

In a similar way than the *per-unit* analysis in power systems, some "base" variables are chosen to make the equations dimensionless. There will be a reference for the time, displacement and voltage which will be the following

$$Z_0 = m_{eq}g/k_{eq}$$

$$T_0 = 2\pi\sqrt{m_{eq}/k_{eq}} = \frac{1}{f_n}$$

$$V_0 = \theta_2 Z_0$$

[5] The matrix presented in this case corresponds to the rectifier circuit in the positive half-cycle. The alterations for the rest of the cases (including the resistive load) can be derived from this case by changing some coefficients.

Now it is possible to redefine the state variables as follows:

$$z^* = \frac{z}{Z_0}$$
$$\frac{dz^*}{dt^*} = \frac{T_0}{Z_0}\dot{z}$$
$$V_x^* = \frac{V_x}{V_0}$$

The corresponding matrices will now be

$$\frac{d}{dt^*}\overrightarrow{x^*} = A^*\overrightarrow{x^*} + B^*\vec{y}^*$$

Where

$$\overrightarrow{x^*} = \begin{bmatrix} z^* \\ dz^*/dt^* \\ V_p^* \\ V_{out}^* \end{bmatrix}$$

$$A^* = \begin{bmatrix} 0 & 1 & 0 & 0 \\ -\frac{k_{eq}}{m_{eq}}T_0^2 & -\frac{c_{eq}}{m_{eq}}T_0 & -\frac{\theta_1}{m_{eq}}\frac{T_0^2}{Z_0 V_0} & 0 \\ 0 & \frac{\theta_2}{1+\frac{C_L}{C_p}}\frac{Z_0}{V_0} & 0 & -\frac{T_0}{R_L(C_L+C_p)} \\ 0 & \frac{\theta_2}{1+\frac{C_L}{C_p}}\frac{Z_0}{V_0} & 0 & -\frac{T_0}{R_L(C_L+C_p)} \end{bmatrix}$$

$$B^* = \begin{bmatrix} 0 & 0 \\ -\frac{c_{air}}{m_{eq}}T_0 & -1 \\ 0 & 0 \end{bmatrix}$$

$$\overrightarrow{y^*} = \begin{bmatrix} \frac{T_0}{Z_0}\dot{y}(t) \\ \frac{T_0^2}{Z_0}\ddot{y}(t) \end{bmatrix}$$

With this formulation, the simulation becomes more robust and convergence will be ensured in most of the cases. After the program solves the equations in the dimensionless domain, the output is converted to the actual physical units to display the results.

Comparison to Experimental Data

The performance of this simulation tool was compared to some published experimental results, especially the ones reported by those references on which the physical model was consulted. In order to evaluate the accuracy of the simulations, the predictions on output voltage (or power) and resonances frequencies were compared for different cases.

A. Erktug (2009)

This is the main reference on which the physical equations are based. The equations were re-derived in this document to apply them to the lumped-parameter model instead of the distributed-parameter model proposed in Erktug's dissertation. The parameters used in the simulation, according to one the experiments done, were the following

Geometry (Bimorph)		**Material (PZT-5H and brass)**		**Circuit**	
Parameter	**Value**	**Parameter**	**Value**	**Parameter**	**Value**
L_b	24.53 mm	Y_s	105 GPa	R_L	(Variable)
L_m[6]	0 mm	c_{11}	60.6 GPa	Rectifier?	0 (false)
t_p	265 µm	e_r^S	2886	Set-up	Series
t_s	140 µm	$\|d_{31}\|$	274 pm/V	**Excitation**	
w	6.4 mm	ρ_s	9000 kg/m^3	Type	Sinusoidal
M_{proof}	2.39E-4 kg	ρ_p	7500 kg/m^3	Amplitude[7]	1.0 g
		η_{loss}	0.0175	Frequency	f_n (varies)

The simulations were performed under two cases: With and without the proof mass in the tip of the beam since both experiments were performed in that reference. The predictions in the resonance frequencies were the following

	Erktug	**nanoHUB**	**Error**
No proof mass			
fsc [Hz]	502.5	510.0	1.5%
foc [Hz]	524.7	538.5	2.6%
Mp = 0.24g			
fsc [Hz]	338.4	341.2	0.8%
foc [Hz]	356.3	360.3	1.1%

The prediction in these frequencies is indeed very accurate. The error compared to the reported data is low enough to make the calculations trustworthy. The following graph shows the comparison to the output voltage predictions compared against the experimental measurements. As indicated in the experimental report, this simulation was performed with a sinusoidal input at constant acceleration (1 *g*) at the short-circuit resonance frequency (i.e. the natural frequency).

[6] In this simulation the "Point mass approximation" was used. This holds because in the experimental set-up the center of gravity of the seismic mass was in the tip of the beam.

[7] In order to ensure that the input acceleration was always 1.0 *g* the amplitude (in meters) was adjustied taking into account the value of the excitation frequency.

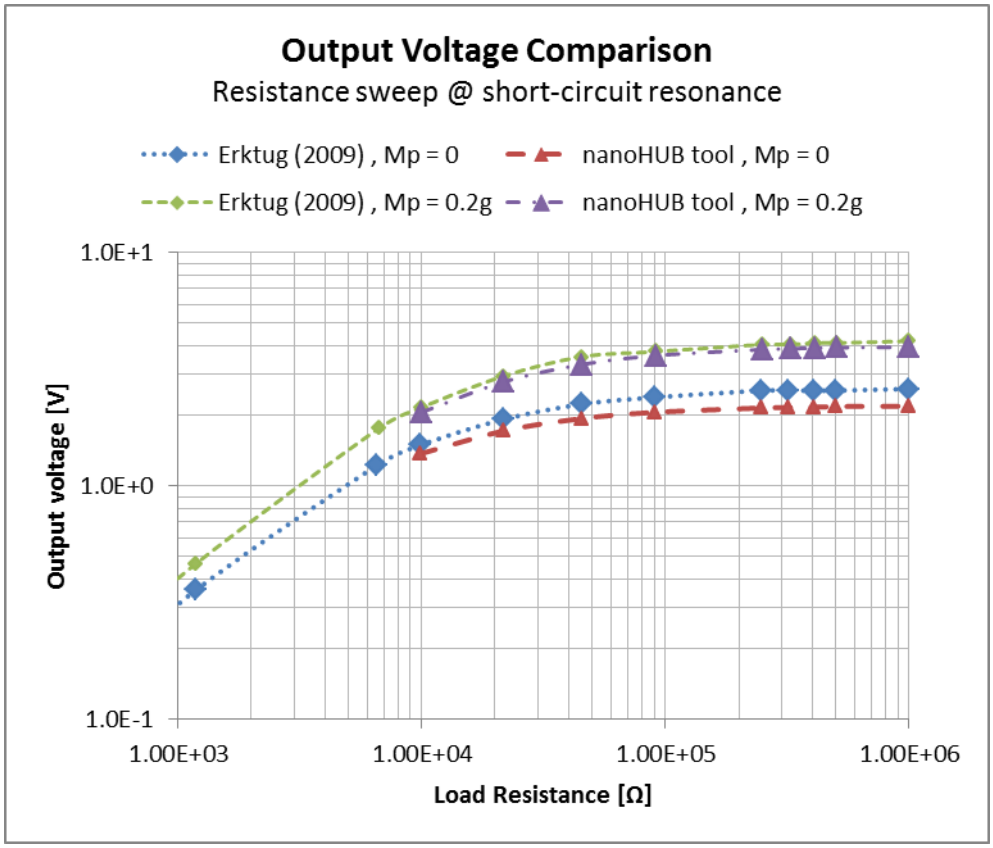

Figure 8 Comparison to Alper Erktug's (2009) experimental data

The calculation of the output voltage for different electrical loads was found to be very accurate for the case with the seismic mass hung in the beam. The graph shows how as the resistance increases, the open-circuit condition is achieved and the voltage reaches a maximum. Both the curve of the experimental data obtained from (Erktug, 2009) and the results of the simulation show the same tendency and show little discrepancy (the error was found to be around 5%). Nonetheless, the simulations without the proof mass were not very accurate, with errors around 15%. This is consistent with the fact that when the inertia is not concentrated at the tip of the beam, the lumped-parameter assumption is not very good. It is important to note that for resistances below 10 kΩ the simulation did not converge. The differential equation became stiff because the RC constant was too low compared to the natural period (T_0), which means that the circuit was very close to the short circuit condition. The results of the simulations with this nanoHUB tool show to be consistent with the experimental data: both at frequency and voltage calculations.

Conclusions

The physical modeling of a MEMS vibrations energy harvesting device has been presented. This model consists of two coupled differential equations which govern the force balance and the electric circuit. Expressions for all the parameters of the differential equations based on the parameters of the materials and the geometry are provided based on the literature available. The simulation of this nanoHUB tool proved to be consistent with the experimental data reported by (Erktug, 2009), especially when there is a proof mass in the cantilevered beam. Hopefully, this simulation program can aid both researchers and students in the understanding and design of piezoelectric vibration scavenging systems.

Future Work

In future versions of this tool, a model should be implemented for the d-33 type and "multi-morph" piezoelectric harvesters. The former ones use interdigitated electrodes to use the d-33 mode of the piezoelectric layers by sections; whereas the latter ones use many substrate and piezoelectric layers. The actual code is extensible to include those features; however, the parameter calculation has to be implemented in a more general way and this would also demand many features to be changed in the interface.

References

Andosca, R., McDonald, T. G., Genova, V., Rosenberg, S., & Keating, J. (2012). Experimental and theoretical studies on MEMS piezoelectric vibrational energy. *Sensors and Actuators*, 76-87.

duTout, N., Wardle, B., & Kim, S.-G. (2005). Design Considerations for MEMS-Scale Piezoelectric Mechanical Vibration Energy Harvesters. *Integrated Ferroelectrics*.

Erktug, A. (2009). *Electromechanical Modeling of Piezoelectric Energy Harvesters.* Virginia Polytechnic Institute and State University.

Hiroshi, H., Kiyoshi, I., & Susumo, K. (1994). Evaluation of Energy Dissipation Mechanism in Vibrational Microactuators. *Micro Electro Mechanical Systems*, 193-198.

Power-Law Viscosity law. (n.d.). Retrieved June 20, 2014, from http://aerojet.engr.ucdavis.edu/fluenthelp/html/ug/node337.htm

Roundy, S. (2003). *Energy Scavenging for Wireless Sensor Nodes with a Focus on Vibration to Electricity Conversion.* University of California, Berkeley.

Townley, A. (n.d.). *Vibrational Energy Harvesting Using MEMS Piezoelectric Generators.* University of Pennsylvania, Electrical Engineering.